The Fracture Mechanical Markov Chain Fatigue Model Compared with Empirical Data

Gansted, L.; Brincker, Rune; Hansen, Lars Pilegaard

Publication date:
1994

Document Version
Publisher's PDF, also known as Version of record

INSTITUTTET FOR BYGNINGSTEKNIK
DEPT. OF BUILDING TECHNOLOGY AND STRUCTURAL ENGINEERING
AALBORG UNIVERSITET • AUC • AALBORG • DANMARK

FRACTURE & DYNAMICS
PAPER NO. 54

L. GANSTED, R. BRINCKER & L. PILEGAARD HANSEN

THE FRACTURE MECHANICAL MARKOV CHAIN FATIGUE MODEL COMPARED WITH EMPIRICAL DATA

OCTOBER 1994 ISSN 0902-7513 R9431

The FRACTURE AND DYNAMICS papers are issued for early dissemination of research results from the Structural Fracture and Dynamics Group at the Department of Building Technology and Structural Engineering, University of Aalborg. These papers are generally submitted to scientific meetings, conferences or journals and should therefore not be widely distributed. Whenever possible reference should be given to the final publications (proceedings, journals, etc.) and not to the Fracture and Dynamics papers.

INSTITUTTET FOR BYGNINGSTEKNIK
DEPT. OF BUILDING TECHNOLOGY AND STRUCTURAL ENGINEERING
AALBORG UNIVERSITET • AUC • AALBORG • DANMARK

FRACTURE & DYNAMICS
PAPER NO. 54

L. GANSTED, R. BRINCKER & L. PILEGAARD HANSEN

THE FRACTURE MECHANICAL MARKOV CHAIN FATIGUE MODEL COMPARED WITH EMPIRICAL DATA

OCTOBER 1994 ISSN 0902-7513 R9431

The Fracture Mechanical Markov Chain Fatigue Model Compared with Empirical Data

Lise Gansted, Rune Brincker and Lars Pilegaard Hansen
Department of Building Technology and Structural Engineering
Aalborg University
Sohngaardsholmsvej 57
DK-9000 Aalborg
Denmark

ABSTRACT

The applicability of the FMF-model (Fracture Mechanical Markov Chain Fatigue Model) introduced in [Gansted, L., R. Brincker and L. Pilegaard Hansen; 1991] is tested by simulations and compared with empirical data. Two sets of data have been used, the Virkler data (aluminium alloy) and data established at the Laboratory of Structural Engineering at Aalborg University, the AUC-data, (mild steel). The model, which is based on the assumption, that the crack propagation process can be described by a discrete space Markov theory, is applicable to constant as well as random loading. It is shown that the FMF-model gives adequate description of the empirical data using model parameters characteristic of the material.

1. INTRODUCTION

Varying loads acting on a structure will cause initiation and propagation of cracks. The cumulative damage (CD) is defined as the irreversible accumulation of damage through lifetime, which ultimately causes fatigue failure. The process is random and justifies reduction of the reliability of the structure.

Some of the consequences of fatigue failure are inconveniences for the users, loss of human life and great economic costs. One way to reduce the risk is to have a mathematical model which is primarily based on physically observable quantities to describe the CD-process.

Usually, distinction is made between two main groups of damage models: deterministic models and probabilistic models.

Deterministic models only give information about the mean damage accumulation, thus ignoring the fluctuations characteristic of fatigue, whereas the use of a probabilistic model makes it possible to take account of the fluctuations and making the CD-model more realistic. The fluctuations are due to variations in the initial state, i.e. distribution of the initial damage e.g. initial crack lengths; variations in the

magnitude and order of load cycles resulting in interaction effects in the form of retardation or acceleration of the crack growth rate and variations the in material properties in the form of e.g. inhomogeneities and loss of isotropy - all of which influence the fatigue crack growth.

The purpose of this paper is to test the applicability of the numerical, probabilistic damage model described in chapter 2. This is done by comparison of empirical fatigue crack growth data with similar simulated data. The simulated data are established from the model, see chapters 3-5.

2. THE BASIC IDEAS OF THE FMF-MODEL

The Fracture Mechanical Markov Chain Fatigue Model (FMF-model) introduced in [Gansted, L., R. Brincker and L. Pilegaard Hansen; 1991] is briefly described in this chapter.

The FMF-model is based on the B-model, see [Bogdanoff, J.L. and F. Kozin; 1985], i.e. on the assumption that the crack propagation process can be described by a discrete space Markov theory. The discrete time is measured as numbers of so-called duty cycles ($x = 1, 2, \ldots$, number of DCs) each consisting of a number of load cycles, and the crack progress is described by a series of discrete damage states ($d = 0, 1, 2, \ldots, b$), where b corresponds to failure.

The damage accumulation is considered as a stochastic process in which the possibility of damage accumulation is present each time the structure has experienced a duty cycle.

It is assumed that the increment of damage at the end of the DC only depends on the DC itself and the state of damage present at the start of the DC. Thus, the history has no influence on the increment, but is included in the state of damage at the start of the DC. The damage only increases by one unit at a time and it is required that the damage measure describes a non-decreasing function.

The damage accumulation can as mentioned be regarded as a discrete-time, discrete-state Markov process which is completely described by its transition matrix (one for each duty cycle) and by the initial conditions.

The damage state at the time x is then given by the vector

$$\overline{p}_x = \overline{p}_0 \, \overline{\overline{P}}_1 \, \overline{\overline{P}}_2 \, \cdots \, \overline{\overline{P}}_x \tag{2.1}$$

where

$\overline{\overline{P}}_i = ((b+1) \times (b+1))$ transition matrix for the ith DC
$\overline{p}_0$ is the initial probability distribution of the damage states
$\overline{p}_x = \{p_x(j)\} = \{\text{prob } \{\text{damage is at the state } j \text{ at the time } x\}\}$

Once the model parameters are determined, the state of damage in the given structure is available at any time using (2.1). This means that all statistical information on the damage process can be represented by the model.

The problem is how to determine the model parameters. In the FMF-model this is done using a fracture mechanical point of view. This is the main point where the FMF-model differs from the B-model in which the parameters are determined solely from empirical data.

The crack length, a, is used as a damage measure which is an advantage since a is a quantity that can easily be observed. The damage is assumed to progress in steps of the length δa. Thus, the jth state of damage can be defined as

$$a_j = a_0 + j\ \delta a \quad ; \quad a_j \leq a_b \quad ; \quad j = 0, 1, 2, \ldots, b \tag{2.2}$$

where

a_j = crack length at the damage state j [mm]
a_0 = initial crack length [mm]
a_b = failure crack length [mm]

The damage process is described by a crack propagation model, expressing the crack growth rate as a function of the fracture mechanical value ΔK, which is the stress intensity factor range, cf. [Hellan, K.; 1985, ch.2].

In agreement with the Markov assumption damage is only accumulated when the crack propagates. As long as the crack remains in a given state, the same test is repeated each time a DC is applied. This means, that at a given crack state, $a = a_j$, the propagation of the crack can be modelled by a Bernoulli random variable Z, see e.g. [Benjamin, J.R. and C.A. Cornell; 1970, p.222], where $z = 0$ corresponds to the crack remains at the given state with the probability $p_j = 1 - q_j$ and where $z = 1$ corresponds to the crack propagates δa with the probability q_j.

The quantity q_j is known as the transition probability. The crack growth problem is then reduced to determination of the transition probability which is a function of the stress intensity factor range, which is a function of the crack state, i.e. $q_j = q(\Delta K_j) = q(\Delta K(a_j))$.

The most simple situation occurs if ΔK is constant, i.e. the crack tip load is constant - thus the applied stress range $\Delta\sigma$ is decreasing - no matter how long the crack is. If so, $\Delta K_j = \Delta K$ and hence, $q_j = q$.

On the basis of the empirical Paris formula, which is one of the most frequently used crack propagation models, and the geometric distribution, estimation of q is possible.

Paris' formula, see [Paris, P.C. and F. Erdogan; 1963], is given as

$$\frac{da}{dN} = C(\Delta K)^m \tag{2.3}$$

where

$$\begin{aligned} da/dN &= \text{crack growth rate [mm/cycle]} \\ C &= \text{material constant [mm/(MPa}\sqrt{\text{m}})^m] \\ m &= \text{material constant} \\ \Delta K &= \text{stress intensity factor range [MPa}\sqrt{\text{m}}] \end{aligned}$$

Empirically, a set of sample curves - (N, a)-curves - is measured. The number of duty cycles N are assumed to be observed for fixed values of the crack length a. Further, the duty cycles are assumed to be equal.

The crack growth rate can be estimated in different ways depending on the definition of the slope of the sample curves. In the FMF-model, the crack growth rate is defined as the crack step length, δa, divided by the mean value of the number of duty cycles, $\mathrm{E}[\delta N]$ applied at a crack state, i.e.,

$$\frac{\delta a}{\mathrm{E}[\delta N]} = \lambda\, C\, (\Delta K)^m \tag{2.4}$$

where

$$\begin{aligned} \mathrm{E}[\delta N] &= \text{the expected value of the random variable } \delta N \text{ corresponding} \\ &\quad \text{to the expected number of duty cycles applied to propagate} \\ &\quad \text{the crack one step } \delta a \\ \lambda &= \text{number of load cycles in one duty cycle} \end{aligned}$$

Notice that the Paris formula has not become stochastic, all quantities in (2.4) are deterministic. (δN is a stochastic variable, but it is $\mathrm{E}[\delta N]$ which is used in (2.4)).

Every time the crack tip is exposed to a duty cycle, the same test is repeated. The expected value and variance of the number of duty cycles performed to propagate the crack δa is to be determined.

It is assumed that for a realization δn of δN the first $(\delta n - 1)$ duty cycles do not lead to crack propagation, i.e. $z = 0$ in (2.6), and that $z = 1$ in the δn th duty cycle, i.e. the δn th duty cycle results in crack propagation. The probability of the two events is $p^{(\delta n - 1)}$ and q, respectively. Thus, the probability distribution of δN is a geometric distribution given as:

$$\mathrm{P}[\delta N = \delta n] = \mathrm{f}_{\delta N}(\delta n) = q\, p^{\delta n - 1} \tag{2.5}$$

The expected value and the variance of the number of duty cycles are given as the first and second moment of the geometric distribution, respectively. Cf. [Benjamin, J.R. and C.A. Cornell; 1970, p.229-230],

$$\mathrm{E}[\delta N] = \sum_{\delta n=0}^{\infty} \delta n\, \mathrm{f}_{\delta N} = \sum_{\delta n=0}^{\infty} \delta n\, q\, (1-q)^{\delta n - 1} = \frac{1}{q} \tag{2.6}$$

$$\mathrm{Var}[\delta N] = \mathrm{E}[\delta N^2] - (\mathrm{E}[\delta N])^2 = \frac{1-q}{q^2} \tag{2.7}$$

The autocovariance is given as the second central moment, see [Benjamin, J.R. and C.A. Cornell; 1970, p.161-162]

$$\mathrm{Cov}[\delta N(t_1, t_2)] = \mathrm{E}[\delta N(t_1)\,\delta N(t_2)] - \mathrm{E}[\delta N(t_1)]\mathrm{E}[\delta N(t_2)] \tag{2.8}$$

where t_1 and t_2 correspond to two different moments, e.g. two successive crack states.

Insertion of (2.6) into (2.4) leads to

$$q = \frac{\lambda C}{\delta a} (\Delta K)^m \tag{2.9}$$

This means, that for a given material the transition matrix (2.2) is determined. The damage states in structures, made of the given material, are then calculated using (2.4). Account of the geometry of the structure is taken through the stress intensity factor range ΔK.

Generally, ΔK is variable due to the load, but in the case of constant-amplitude load (stress range $\Delta\sigma$ constant) ΔK can be assumed constant in the vicinity of the given crack position.

At each crack position, given by (2.2), the random variable δN_j, which is the number of duty cycles applied to propagate the crack one step from a_j to $a_j + \delta a$, is considered. It is assumed that a_0 is constant so that the δN_j-values express the properties of the material.

Similar to the results for ΔK constant, the first $(\delta n_j - 1)$ duty cycles with the probability $p_j^{(\delta n_j - 1)}$ do not lead to crack propagation, whereas the δn_j th duty cycle with probability q_j results in crack propagation. Thus, the probability distribution of δN_j is a geometric distribution given as:

$$\mathrm{P}[\delta N_j = \delta n_j] = \mathrm{f}_{\delta N_j}(\delta n_j) = q_j\, p_j^{\delta n_j - 1} \qquad j = 0, 1, 2, \ldots, b-1 \tag{2.10}$$

where the expected value, the variance and the autocovariance of δN_j are given by (2.6)-(2.8) replacing δN and q by δN_j and q_j, i.e.

$$\mathrm{E}[\delta N_j] = \frac{1}{q_j} \tag{2.11}$$

$$\mathrm{Var}[\delta N_j] = \frac{1-q_j}{q_j^2} \tag{2.12}$$

$$\mathrm{Cov}[\delta N_j(t_1,t_2)] = \mathrm{E}[\delta N_j(t_1)\,\delta N_j(t_2)] - \mathrm{E}[\delta N_j(t_1)]\mathrm{E}[\delta N_j(t_2)] \tag{2.13}$$

where

$$q_j = \frac{\lambda C}{\delta a}\,(\Delta K(a_0 + j\delta a))^m = \frac{\lambda C}{\delta a}\,(\Delta K(a_j))^m \tag{2.14}$$

$$p_j = 1 - q_j$$

The total number of duty cycles applied to a structure to propagate the crack to the crack length a_j is

$$N_j = \sum_{k=0}^{j-1} \delta N_k \tag{2.15}$$

Since the random variable is a sum of independent random variables, the expected value of the number of duty cycles is

$$\mathrm{E}[N_j] = \mathrm{E}\left[\sum_{k=0}^{j-1} \delta N_k\right] = \sum_{k=0}^{j-1} \frac{1}{q_k} \simeq \frac{1}{\lambda C}\int_{a_0}^{a_j} (\Delta K(a))^{-m}\,da \tag{2.16}$$

where the sum is approximated by an integral.

The variance of a sum of independent variables is given as, see e.g. [Benjamin, J.R. and C.A. Cornell; 1970, p.227]

$$\mathrm{Var}[N_j] = \sum_{k=0}^{j-1} \mathrm{Var}[\delta N_k] = \sum_{k=0}^{j-1} \frac{1-q_k}{q_k^2} = \frac{\delta a}{\lambda^2 C^2}\,[f(a) - g(a)] \tag{2.17}$$

where the sum is approximated by an integral and where

$$f(a) = \int_{a_0}^{a_j} (\Delta K(a))^{-2m}\,da \tag{2.18}$$

$$g(a) = \frac{\lambda C}{\delta a}\int_{a_0}^{a_j} (\Delta K(a))^{-m}\,da \tag{2.19}$$

Finally, the autocovariance is given as

$$\mathrm{Cov}[N_j(t_1,t_2)] = \mathrm{E}[N_j(t_1)\,N_j(t_2)] - \mathrm{E}[N_j(t_1)]\mathrm{E}[N_j(t_2)] \tag{2.20}$$

The only unknown quantity left is the step length δa, which can be estimated if the variance of N_j (or the variance of $\lambda^2 N_j$, i.e. of the number of load cycles) is known from experiments, see [Gansted, L.; 1993].

In case of random load, the stress intensity factor will also vary randomly and the well-known effects of acceleration and retardation might occur. The FMF-model itself does not take account of these interaction effects. This can be done using a crack closure model when ΔK is calculated, see e.g. [Schijve, J.; 1979] and [Corbly, D.M. and P.F. Packman; 1973].

The damage increment in the next duty cycle will depend on the load history, the geometry of the structure and the extreme values of the duty cycle.

Introducing the effective stress intensity factor range,

$$\Delta K_{\text{eff}} = \Delta\sigma_{\text{eff}} F \sqrt{\pi a} = (\sigma_{\max} - \sigma_{cl}) F \sqrt{\pi a} \tag{2.21}$$

where

$\Delta\sigma_{\text{eff}}$	=	effective stress range [MPa]
$\sigma_{\max}$	=	maximum stress [MPa]
σ_{cl}	=	crack closure stress [MPa]
F	=	geometry function
a	=	crack length

The FMF-model is also available if the load is random. The only changes to be made are to replace ΔK by ΔK_{eff} in (2.3), (2.4), (2.9), (2.14), (2.16), (2.18) and in (2.19).

Hereby, the basic ideas of the FMF-model are introduced.

3. TEST OF THE FMF-MODEL

In this chapter it is described how the FMF-model is tested for the purpose of evaluation of its applicability and to test if δa can be regarded as a characteristic value of the material.

This evaluation is based on the following criteria concerning the properties of the model.

Firstly, the model must be able to give a good qualitative description of empirical crack growth curves, i.e. the model can replicate the empirical curves. Secondly, the crack growth data obtained from the model must have the same statistical properties as the empirical data in the form of mean values, standard deviations, autocovariances and probability density functions.

The qualitative demand is tested by plotting the crack growth curves obtained from the model and from the empirical data, respectively. The curves must show similar

form and progress.

The quantitative tests are performed by using several C-programs developed in connection with the FMF-model. Further, the most well-known set of data originating from several experiments, i.e. the Virkler data, has been used in the tests as reference. The Virkler data, which have been available to the author in their original form, are described in [Bogdanoff, J.L and F. Kozin; 1985, ch.4] and [Virkler, D.A., B.M. Hillberry and P.K. Goel; 1979], see chapter 4. Further, the AUC-data established at the Laboratory of Structural Engineering at Aalborg University have been used in chapter 5.

The test procedure is described in the following.

Firstly, simulations of (N, a)-data on the basis of the FMF-model are performed knowing the initial and the critical crack length (a_0 and a_{cr}), the stress range ($\Delta\sigma$) and the number of cycles in each duty cycle (λ) besides the experimentally determined material constants C and m. All these values are fixed. The only parameter which is variable is the crack step length δa. The number of data set in each simulation series is 500.

Secondly, the simulated (N, a)-values are used to calculate the mean value and the standard deviation of the number of cycles applied at each crack state to reach the successive state and of the number of cycles applied totally to reach a given crack state, i.e. the values of (2.11), (2.12), (2.16) and (2.17).

Besides, the autocovariance of the crack growth rate da/dN as a function of a is calculated for three different crack states.

Finally, these statistical values are to be compared with the corresponding values obtained on the basis of the Virkler data and the AUC-data, respectively.

4. THE FMF-MODEL APPLIED TO THE VIRKLER DATA

In this chapter the tests described in chapter 3 are performed applying the FMF-model to the Virkler data. Firstly, the Virkler data are introduced, secondly, the simulated data are established and finally, a comparison based on the criteria mentioned in chapter 3 is performed.

4.1 The Virkler Data

The purpose of this section is to give a description of the fatigue crack growth data used as references in the numerical test of the FMF-model.

The Virkler data - shown in figure 4.1 - were obtained from 68 tests using 2024-T3 aluminium alloy CCT-specimens (Center Cracked Tension). The size of the CCT-specimens was $152.4 \cdot 558.8$ mm^2 ($6 \cdot 22$ in^2) with a thickness of 2.54 mm (0.10 in).

No specification of the material properties has been found. The CCT-specimens were influenced by constant-amplitude load with stress range $\Delta\sigma = 48.28$ MPa, maximum stress $\sigma_{\max} = 60.35$ MPa and minimum stress $\sigma_{\min} = 12.07$ MPa.

In each test, 164 values of the number of cycles and the crack length, (N, a), were recorded for fixed values of the increase of the crack length, da. For $a \in [9.0\ ;\ 36.2]$ mm, $da = 0.20$ mm where $a_0 = 9.0$ mm is the initial crack length. For $a \in [36.2\ ;\ 44.2]$ mm, $da = 0.40$ mm and finally, $da = 0.80$ mm for $a \in [44.2\ ;\ 49.8]$ mm where $a_f = 49.8$ mm is the failure crack length.

The crack lengths were measured by a zoom stereo microscope operated at a magnification of 150×. The microscope was mounted on a digital traversing system with a resolution of 0.001 mm. Illuminating the crack with a strobe light, measuring of the crack length was possible without interrupting the loading.

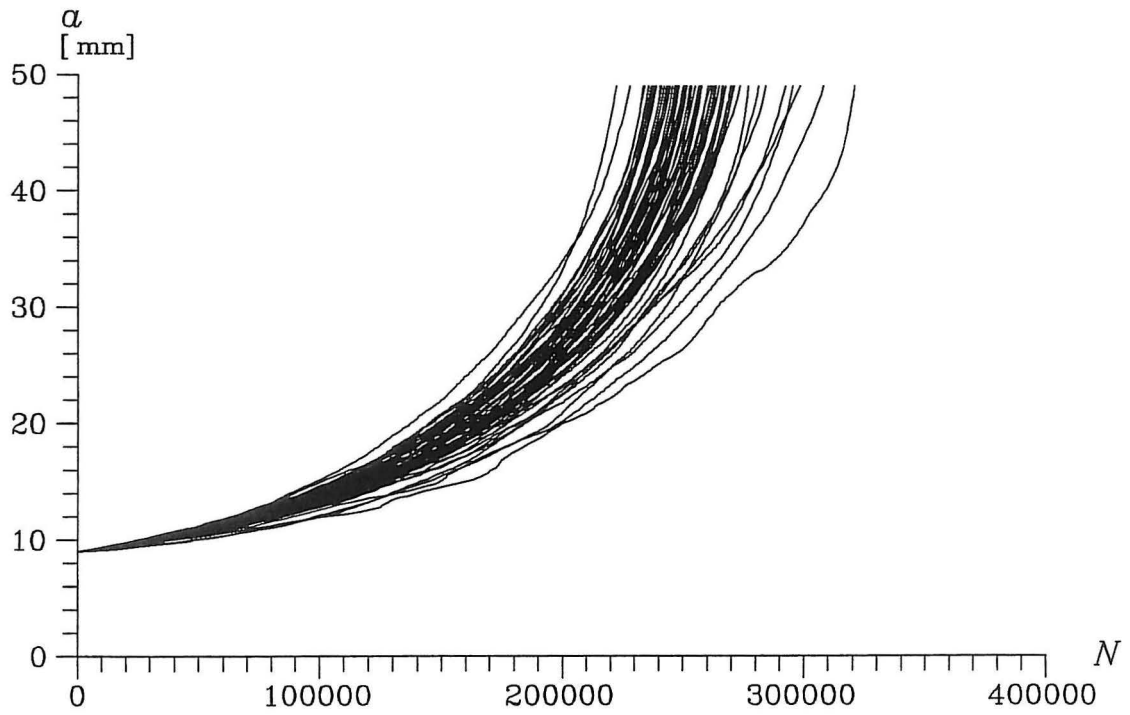

Figure 4.1: The 68 (N, a)-curves obtained from the Virkler data.
N = number of load cycles, a = crack length.
Based on [Bogdanoff, J.L. and F. Kozin; 1985, p.241].

The form of the curves in figure 4.1 shows great similarity. Thus, all the curves have a smooth progress with only a few sudden changes in the crack growth rate. Further, the curves approach a vertical line for large a-values corresponding to only a few number of cycles being applied in the last part of the fatigue failure. This approach would have been even more significant if the measurings were continued until final rupture occured.

It is seen that a large initial crack growth rate results in a small number of cycles to cause failure and vice versa. Further, the main part of the curves is concentrated

within a small band where $N_f \in [230000\ ;\ 270000]$ cycles.

4.2 Simulated FMF-Data with Virkler Parameters

For the purpose of testing the FMF-model (N, a)-data (N = number of cycles, a = crack length) are simulated on the basis of the FMF-model. The number of data set in each simulation series is 500.

The input parameters shown in table 4.2 are kept constant corresponding to the Virkler data. The initial crack length a_0, the failure crack length a_f and the stress range $\Delta\sigma$ are explicitly known from [Virkler, D.A., B.M. Hillberry and P.K. Goel; 1979], whereas C and m are determined by the authors on the basis of the original Virkler data.

a_0 [mm]	a_f [mm]	$\Delta\sigma$ [MPa]	C [mm/(MPa$\sqrt{\text{m}}$)$^{3.73}$]	m	λ
9.0	49.8	48.28	$1.26 \cdot 10^{-8}$	3.73	1

Table 4.2: Input parameters for simulation series VSIM A and VSIM B. a_0 = initial crack length, a_f = failure crack length, $\Delta\sigma$ = stress range, C = material constant, m = material constant and λ = number of load cycles in each duty cycle.

The remaining parameter δa (crack step length) is varied. The δa used for the simulations of FMF-data is shown in table 4.3.

	δa [mm]
VSIM A	0.2
VSIM B	0.1

Table 4.3: The δa values used in the simulation series VSIM A and VSIM B.

An example of (N, a)-curves from the simulation series are shown in figures 4.4 and 4.5. For simplicity, only 100 of the 500 simulated (N, a)-curves are shown in the plot. The curves have been plotted successively, i.e. the plot contains the first 100 curves.

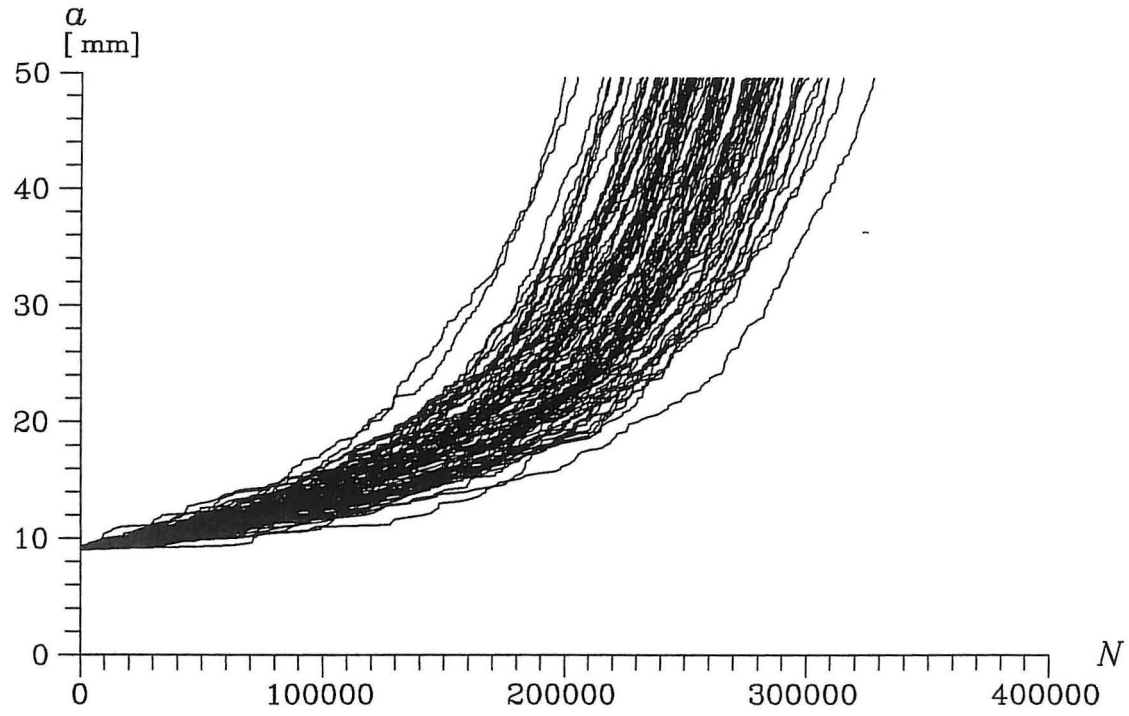

Figure 4.4: Typical plot of (N, a)-curves from simulation series VSIM A.
N = number of load cycles, a = crack length.

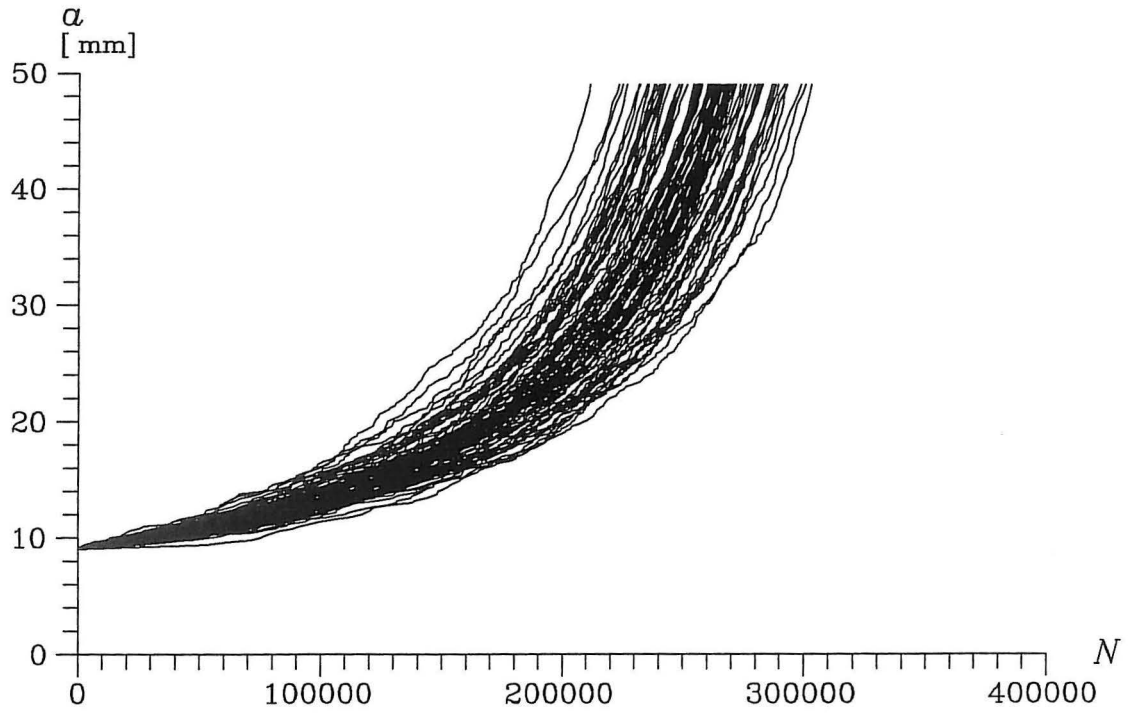

Figure 4.5: Typical plot of (N, a)-curves from simulation series VSIM B.
N = number of load cycles, a = crack length.

A qualitative evaluation of figures 4.4 and 4.5 shows that the (N, a)-curves have almost the same characteristics as the curves in figure 4.1 for the Virkler data.

The smoothness of the curves increases as δa decreases. Thus, for simulation series VSIM A (figure 4.4), the curves have a less smooth progress compared to simulation series VSIM B (figure 4.5).

This is caused by the fact that in simulation series VSIM A the crack is forced to propagate in steps of 0.2 mm, whereas in simulation series VSIM B the steps are 0.1 mm.

As for the Virkler data it is seen that a large initial crack growth results in a small number of cycles to cause failure and vice versa. The main part of the curves has the failure number of cycles concentrated within the interval $N_f \in [200000 ; 300000]$.

A quantitative evaluation of the simulation results is given in section 4.3.

4.3 Comparison of Virkler Data and Simulated FMF-Data

For the purpose of evaluating how well the FMF-model is able to describe fatigue crack growth, the statistical properties are compared with the similar values of the Virkler data.

The results from the simulation series, in the form of related (N, a)-values (see figures 4.4 and 4.5), are used as input parameters to calculate the statistical properties mentioned in chapter 3. Only the data corresponding to the crack lengths used in the Virkler data are selected.

The total number of cycles to reach the failure state N_f and the deviation of the total number of cycles to reach a crack state $S_{N_j} = (\mathrm{Var}[N_j])^{1/2}$ are considered to be the most important statistical properties together with the autocovariance of the crack growth rate da/dN as a function of a.

This considering that, by observation of a given crack length the primary requirement is to be able to predict the number of load cycles, which can be further applied before the failure state (or any other state) is reached.

This is the reason why these are the only curves shown in this paper, see figures 4.6-4.10. The remaining curves can be seen in [Gansted, L.; 1991]. All statistical values are used in the numerical comparison later in this section.

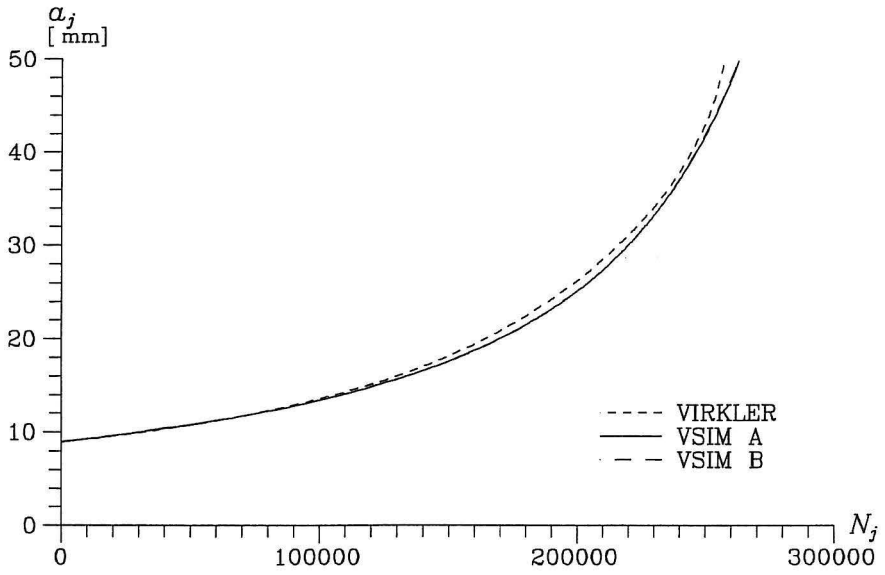

Figure 4.6: Mean value of the number of load cycles ($\overline{N}_j$) applied to reach the crack state (a_j), for the Virkler data, VSIM A and VSIM B. $j = 0, 1, 2, \ldots, 163$, $a_0 = 9.0$ mm and $a_{163} = 49.8$ mm.

Even though the (N, a)-curves in figures 4.4 and 4.5 have some variations in their progress, the mean value of the number of load cycles $\overline{N}_j$ applied to reach a crack state a_j describes a very smooth non-decreasing function, see figure 4.6. The mean number of cycles to cause failure $\overline{N}_f = \overline{N}_{163} \approx 260000$ cycles which is the same as found for the Virkler data in figure 4.1.

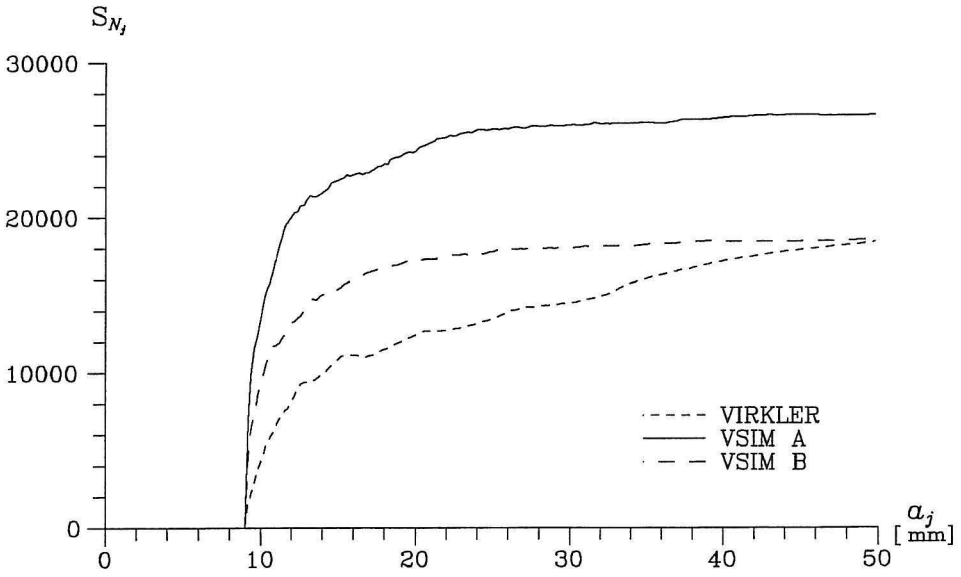

Figure 4.7: Standard deviation of the number of load cycles (S_{N_j}) applied to reach the crack state (a_j) for the Virkler data, VSIM A and VSIM B. $j = 0, 1, 2, \ldots, 163$, $a_0 = 9.0$ mm and $a_{163} = 49.8$ mm.

The standard deviation of the number of load cycles S_{N_j} applied to reach the crack state a_j is increasing for increasing crack length, see figure 4.7. The increase is largest for small crack lengths ($a < 12$ mm) after which the standard deviation slowly increases towards its maximum value of ≈ 20000 cycles for the Virkler data. The simulated data seems to reach a constant value at a relatively early stage and the constant value in the simulation series is seen to be influenced by δa. Thus, for $\delta a = 0.2$ mm (VSIM A) $S_{N_j} \approx 28000$ cycles and for $\delta a = 0.1$ mm (VSIM B) $S_{N_j} \approx 18000$ cycles.

The relative deviation varies for the Virkler data from $\approx 10\%$ for small crack lengths to $\approx 7\%$ for large crack lengths. Likewise, the relative deviation varies from $\approx 20\%$ for small crack lengths to $\approx 8\%$ for large crack lengths for the simulation series.

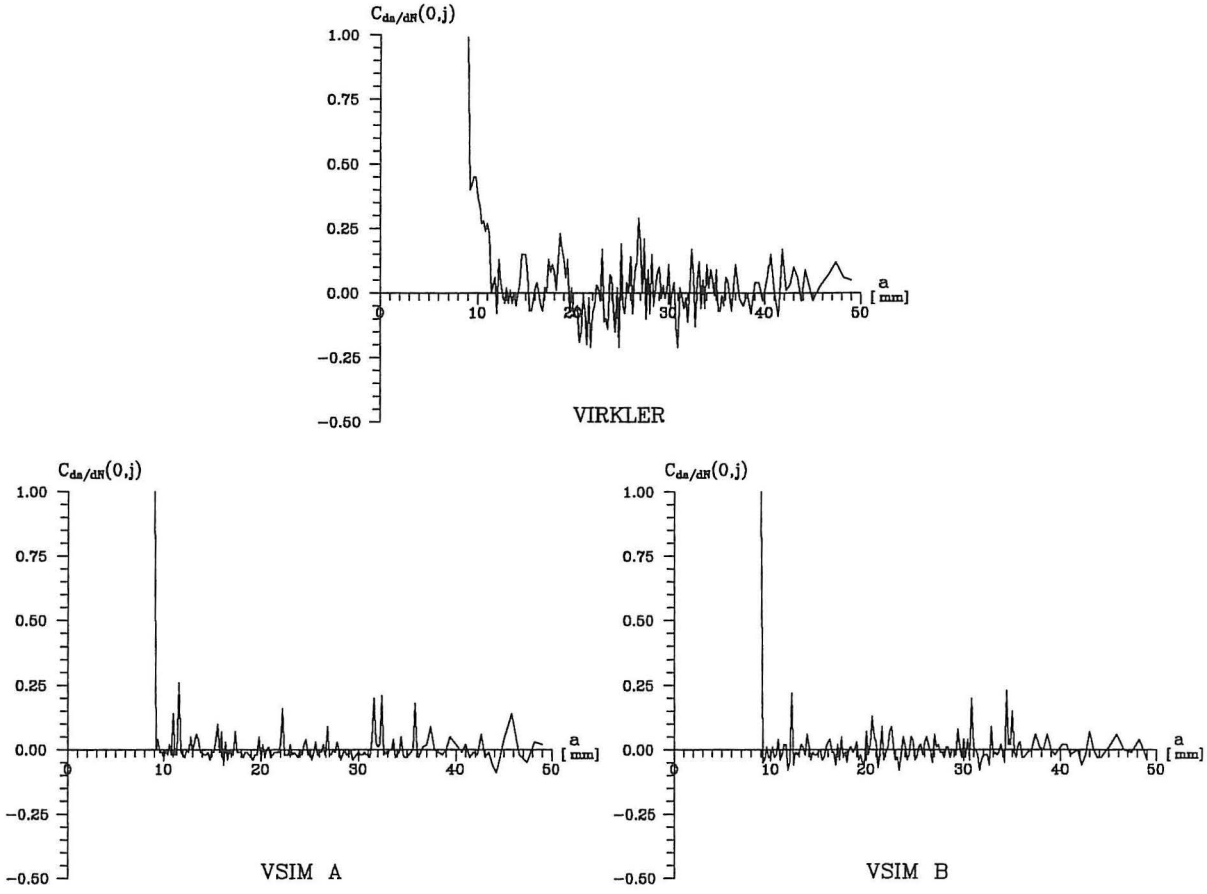

Figure 4.8: Autocovariance of the crack growth rate ($C_{da/dN}$) at the crack state a_0 = 9.0 mm for the Virkler data, VSIM A and VSIM B, respectively.

The progress of the three curves for $C_{da/dN}(0, j)$ in figure 4.8, shows the same tendency. Thus, the curves start with a peak value = 1 and for $a > a_0$ the curves fluctuate around zero.

The autocovariance $C_{da/dN}(0, j)$ for the Virkler data has larger fluctuations concentrated within the interval [-0.20 ; 0.25] than the curves for VSIM A and VSIM B, respectively. The two last-mentioned curves are concentrated within the interval

[-0.075 ; 0.20].

The difference between the Virkler data and the simulated data might be due to the difference in number of curves (68 and 500, respectively).

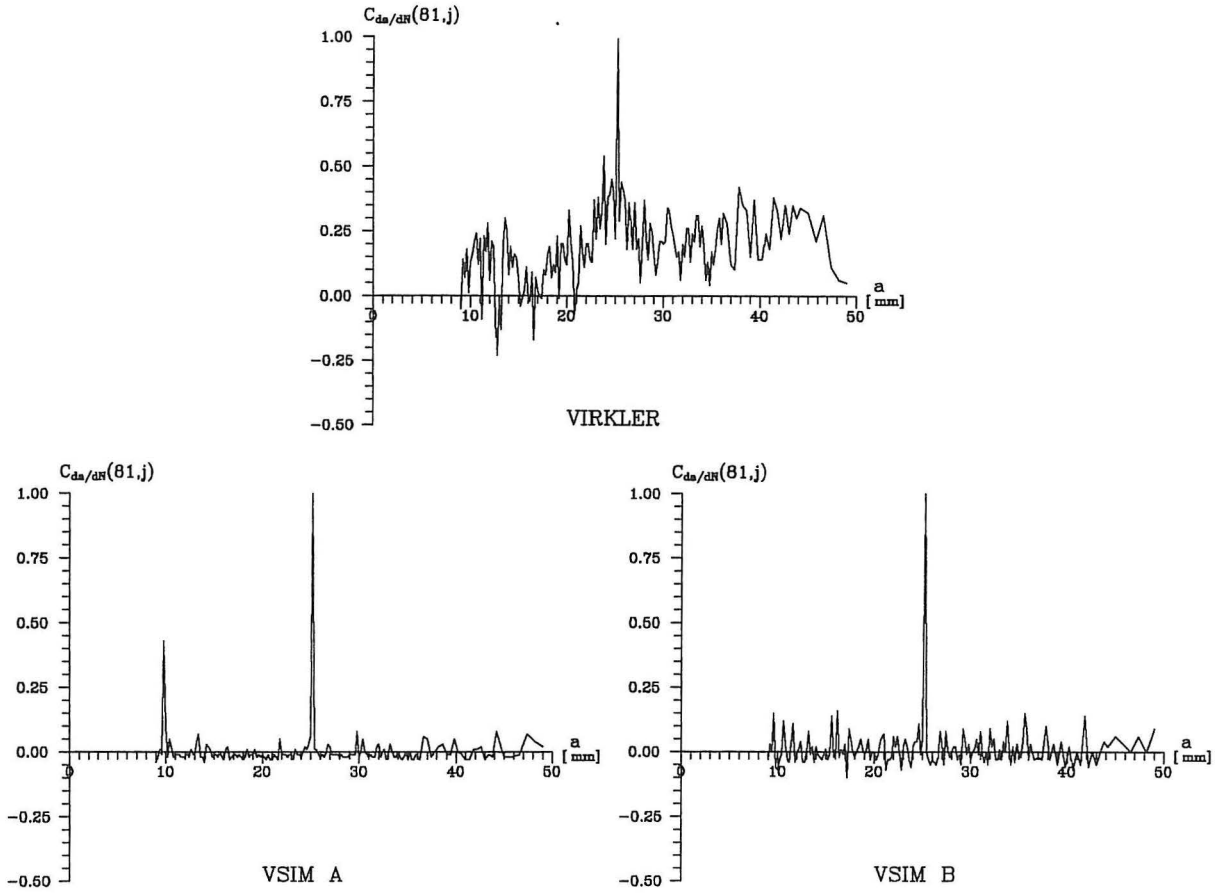

Figure 4.9: Autocovariance of the crack growth rate ($C_{da/dN}$) at the crack state a_{81} = 25.2 mm for the Virkler data, VSIM A and VSIM B, respectively.

The autocovariance $C_{da/dN}(81, j)$ for the Virkler data shown in figure 4.9 differs from the one in figure 4.8. Thus the mean value varies with varying crack length starting with approximately 0.10 and ending with approximately 0.25. This means that the crack growth rate da/dN at the crack state a_{81} = 25.4 mm is influenced by da/dN for $a < a_{81}$ and that da/dN for $a > a_{81}$ depends on the crack growth rate for a_{81} = 25.4 mm.

Except for the small peak at a_4 = 9.80 mm, the progress of $C_{da/dN}(81, j)$ for VSIM A is characterized by small fluctuations around zero and with the peak value = 1 for a_{81} = 25.4 mm. The same tendency is seen for VSIM B only with larger, but still small, fluctuations within the interval [-0.10 ; 0.15].

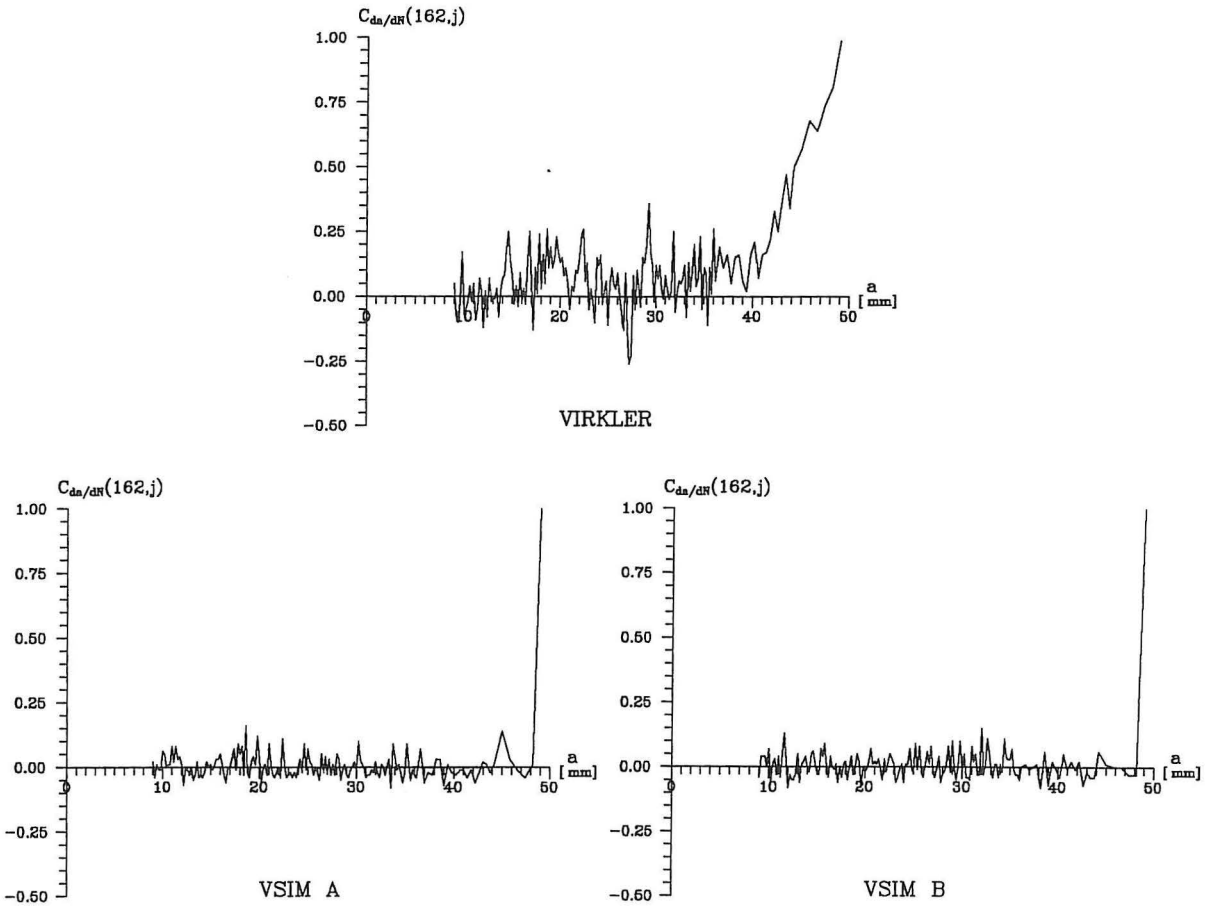

Figure 4.10: Autocovariance of the crack growth rate ($C_{da/dN}$) at the crack state a_{162} = 49.0 mm for the Virkler data, VSIM A and VSIM B, respectively.

In figure 4.10 it is seen that the autocovariance $C_{da/dN}(162, j)$ for the Virkler data is concentrated within the interval [-0.15 ; 0.25] with increasing mean value for $a > a_{151}$ = 42.2 mm until the peak value = 1 is reached at a_{162} = 49.0 mm.

Neither for VSIM A nor for VSIM B the crack growth rate at the crack state a_{162} = 49.0 mm is influenced by the crack growth rate at the previous crack states. Thus $C_{da/dN}(162, j)$ fluctuates within the interval [-0.05 ; 0.10] with a small positive mean value.

The numerical comparison of the statistical values is based on the following norm, which is applied to each of the statistical properties mentioned in chapter 3.

$$q_X = \left[\sum_{j=0}^{n} (x_{\text{VSIM}} - x_{\text{VIRKLER}})^2 \right]^{\frac{1}{2}} \tag{4.1}$$

where

X = the statistical property in consideration

n = 162 for δN_j and 163 for N_j
x_{VSIM} = statistical value of VSIM A and VSIM B
x_{VIRKLER} = statistical value of the Virkler data

The results of the calculations are given in table 4.21.

	$q_{\overline{\delta N_j}}$ (10^6)	$q_{S_{\delta N_j}}$ (10^8)	$q_{Q_{\delta N_j}}$ (10^6)	$q_{\overline{N}_j}$ (10^9)	$q_{S_{N_j}}$ (10^9)	$q_{Q_{N_j}}$ (10^6)	$q_{C_{da/dN}}$
VSIM A	5.1	4.5	4.2	2.6	20.1	3.8	113.9
VSIM B	4.3	1.7	4.0	2.5	2.5	5.4	108.3

Table 4.11: Norm values q for: mean value ($\overline{\delta N}_j$), standard deviation ($S_{\delta N_j}$) and probability density ($Q_{\delta N_j}$) of the number of load cycles applied at each crack state (a_j); mean value ($\overline{N}_j$), standard deviation (S_{N_j}) and probability density (Q_{N_j}) of the number of load cycles applied to reach a crack state (a_j); autocovariance of the crack growth rate ($C_{da/dN}$) for three different crack lengths. The norm values are calculated for simulation series VSIM A and VSIM B (see table 4.3) using the Virkler data as reference.

The purpose is that the parameter δa in the FMF-model have such value that the statistical properties of the simulated FMF-data correspond to the similar properties of the Virkler data, i.e. the q-values should be as small as possible.

In table 4.11 it is seen that in general, the q-values are higher for VSIM A than for VSIM B and that there is a significant difference between the q-values for S_{N_j}. Thus, the value for VSIM A are approximately 8 times the value for VSIM B, i.e. the value of δa has a decisive influence on how well the crack growth data are described by the FMF-model.

The difference between VSIM A on one side and VSIM B and the Virkler data on the other side, is also seen by comparison of the curves in figure 4.7. The curve for VSIM A generally assumes larger values than the curve for the Virkler data and thus they are responsible for the high q-value for S_{N_j} in table 4.11.

The lower q-values for S_{N_j} for VSIM B are due to the fact that the S_{N_j}-curve for VSIM B is placed at the same level as the curve for the Virkler data. The difference between the curves is seen especially for small a-values, whereas the same final value is approached asymptotically.

Thus, it might be concluded that the Virkler data are best described by the FMF-model using $\delta a = 0.1$ mm.

Bearing in mind that N_j is the number of DCs, it can be shown - see e.g. [Gansted, L.; 1991, ch.5] - that (2.17) leads to

$$S_{N_f} \approx \frac{a_0^{1/2}\,(10^3)^{m/2}}{C\,(\Delta\sigma\,\sqrt{\pi\,a_0})^m\,(m-1)^{1/2}\,(\delta a)^{1/2}} \tag{4.2}$$

which is the standard deviation of the number of load cycles to cause failure, S_{N_f}, where the initial crack length a_0 and the crack step length δa are measured in [mm], the material parameter C in [mm/(MPa$\sqrt{\text{m}}$)^m] and the stress range $\Delta\sigma$ in [MPa]. The factor $(10^3)^{m/2}$ is necessary to obtain consistency in dimensions.

Using the values from table 4.2 in (4.2), the standard deviation of N_f can be calculated as a function of δa. This is illustrated in figure 4.12.

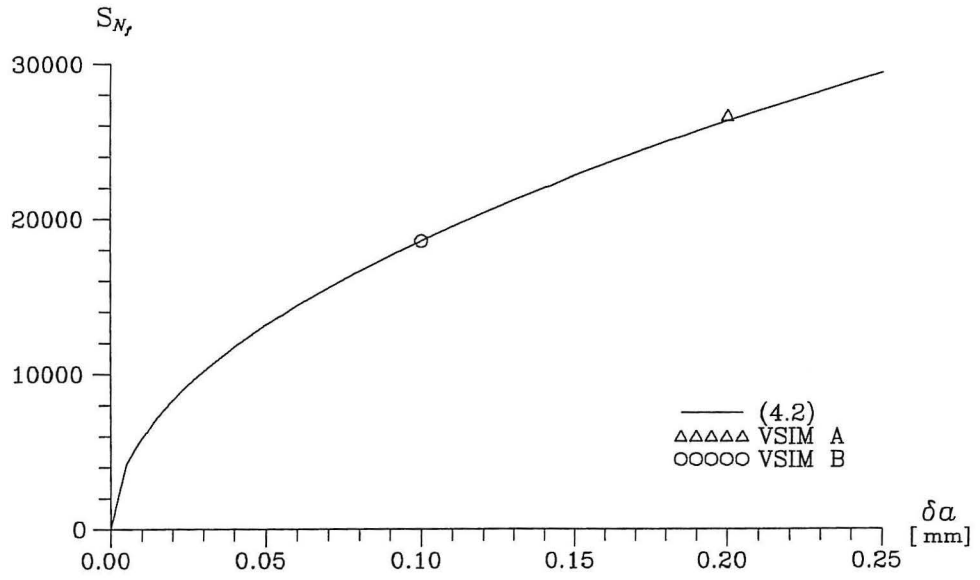

Figure 4.12: Standard deviation of the number of load cycles to cause failure as a function of the crack step length. The S_{N_f}-values for VSIM A and VSIM B are also seen in figure 4.7.

Figure 4.12 shows good agreement between (4.2) and the simulation series VSIM A and VSIM B.

As a consequence of the agreement between the analytical expression (4.1) and the numerical results, the most appropriate estimate of δa can be found (4.2) on the basis of the S_{N_f}-value for the Virkler data, i.e.

$$\delta a = \frac{C^2\,(\Delta\sigma\,\sqrt{\pi\,a_0})^{2m}\,(m-1)}{a_0\,(10^3)^m}\,S_{N_f}^2 \tag{4.3}$$

Insertion of the values from table 4.2 and $S_{N_f} = 18446.80$ cycles (see figure 4.6) results in $\delta a = 0.0983$ mm as an estimate of the δa-value giving the best description of the Virkler data. The value used in the simulations VSIM B ($\delta a = 0.1$ mm) roughly corresponds to the analytical estimation ($\delta a = 0.0983$ mm) so no further calculations will be made.

It should be noted that δa is strongly dependent on the applied S_{N_f}-value - and thus on the failure crack length a_f. This can be seen in figure 4.6 in which S_{N_j} as a function of a_j is illustrated for the Virkler data, VSIM A and VSIM B, respectively.

Figure 4.7 shows that for $a_j < a_f$, S_{N_j} for the simulated data deviates from S_{N_j} for the Virkler data. In this case, the δa-value determined by (4.3), where S_{N_j} is inserted, will not give an adequate description of the Virkler data. It should be noted that (4.3) are established on the assumption that $a_f \gg a_0$.

The evaluation of the FMF-model on the basis of the numerical results is performed in chapter 6.

5. THE FMF-MODEL APPLIED TO THE AUC-DATA

The experimental tests described in the present chapter serve two purposes: a) The model parameters used in the FMF-model are determined for a mild steel. b) Reference data for the evaluation of the applicability of the FMF-model are established.

5.1 The AUC-Data

The AUC-data - shown in figure 5.1 - were obtained from 34 tests using STW22 DIN 1614 steel CCT-specimens (Center Cracked Tension). The size of the CCT-specimens was $80 \cdot 180$ mm^2 with a thickness of 2.5 mm. The material specifications are given in [Gansted, L.; 1993]. The CCT-specimens were influenced by constant-amplitude load with stress range $\Delta\sigma = 125$ MPa, maximum stress $\sigma_{\max} = 127.5$ MPa and minimum stress $\sigma_{\min} = 2.5$ MPa.

In each test, the number of load cycles and the crack length (N, a) were recorded for fixed values of δN by use of the DIP technique (Digital Image Processing). At the beginning of each test δN is chosen as 5000 cycles and when the crack growth rate increases, δN is divided into halves until $\delta N = 625$ cycles, as a minimum.

On the basis of figure 3.1, the material parameters C and m in (2.14) are found to assume the values $2.5075 \cdot 10^{-9}$ mm/(MPa$\sqrt{\text{m}}$)^m and 3.486, respectively - see also [Gansted, L.; 1991].

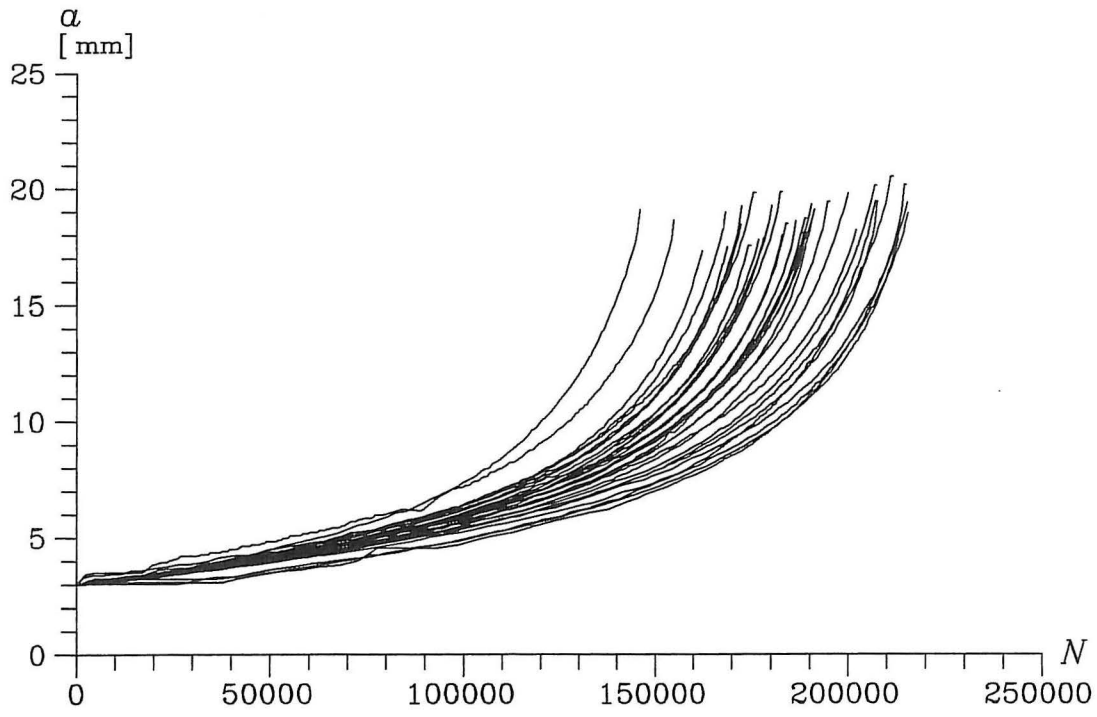

Figure 5.1: The 34 (N, a)-curves obtained from the AUC-data established at the Laboratory of Structural Engineering at Aalborg University.
N = number of load cycles, a = crack length. After [Gansted, L.; 1993].

The FMF-model requires that δa and not δN is a fixed parameter, but this is not yet possible with the DIP technique, and other available methods are much more resource demanding. In the statistical analysis of the (N, a)-data, interpolation is used in order to obtain fixed δa-values. Thus, for $a \in [3.0\ ;\ 17.5]$ mm, $\delta a = 0.10$ mm where $a_0 = 3.0$ mm is the initial crack length and where $a_f = 17.5$ mm is the failure crack length.

Thus, all the model parameters used in the FMF-model are determined.

5.2 Simulated FMF-Data with AUC-Parameters

For the purpose of evaluating the applicability of the FMF-model simulations of (N, a)-data are performed on the basis of the FMF-model. The simulations are described in this section.

The model parameters used in the FMF-model are found in section 5.1 and summarized in table 5.2. The crack step length is established using (4.3). Insertion of a_0, $\Delta\sigma$, C, m and $S_{N_f} = 17115$ (see figure 5.4) leads to $\delta a = 0.0552$ mm.

a_0 [mm]	a_f [mm]	$\Delta\sigma$ [MPa]	C [mm/(MPa$\sqrt{\text{m}}$)^m]	m	λ	δa [mm]
3.0	17.5	125	$2.5075 \cdot 10^{-9}$	3.486	1	0.0552

Table 5.2: Input parameters for the simulation series.
a_0 = initial crack length, a_f = failure crack length, $\Delta\sigma$ = stress range, C = material constant, m = material constant, λ = number of load cycles in each duty cycle and δa = crack step length.

The number of data sets in a simulation series is 500, but only 100 curves are shown in figure 5.3.

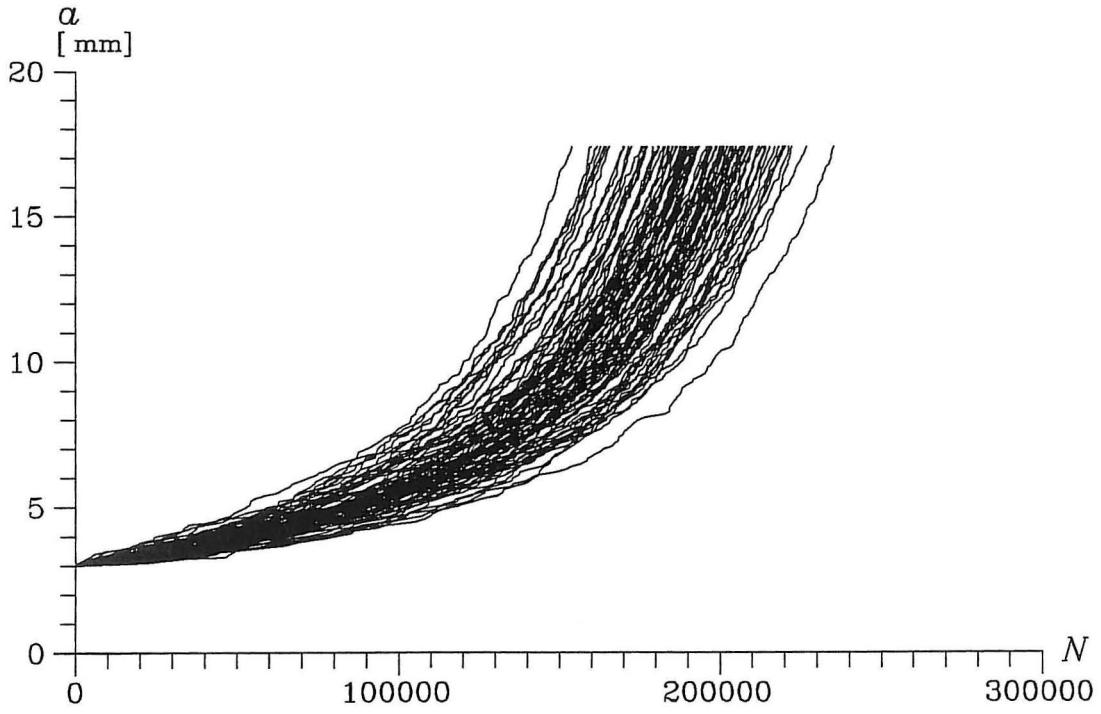

Figure 5.3: (N, a)-curves obtained by simulations on the basis of the FMF-model with model parameters as given in table 5.2.
N = number of load cycles, a = crack length.

The qualitative demand is tested by plotting the fatigue crack growth curves obtained from the empirical data and from the simulated data, respectively. The curves must have similar form and progress.

The fatigue crack growth curves are shown in figures 5.1 and 5.3. It is seen that the simulated data have a less smooth progress than the AUC-data, but almost the same form. Thus, a small initial crack growth rate results in a large number of cycles to cause failure and vice versa. Further, the curves approach a vertical line for large a-values corresponding to only a few cycles in the last part of the fatigue failure.

5.3 Comparison of AUC-Data and Simulated FMF-Data

In this section the applicability of the FMF-model is evaluated on the basis of the AUC-data and on the criteria mentioned in chapter 3 concerning the properties of the model.

As in section 4.3, the results from the simulation series are used to calculate the statistical values of the simulated data. Only the curves for the standard deviation of the total number of cycles to reach a crack state $S_{N_j} = (\mathrm{Var}[N_j])^{1/2}$ are shown together with the autocovariance of the crack growth rate da/dN as a function of the crack length a. See also comments in section 4.3.

The main part of the empirical curves is concentrated within the interval $N_f \in [150000 ; 200000]$ cycles, whereas for the simulated data $N_f \in [160000 ; 225000]$ cycles, i.e. a small displacement, but with a large overlap. The mean values of N_f are 185353 cycles for the AUC-data and 198779 cycles for the simulated data, respectively.

The progress of S_{N_j} is shown in figure 5.4 for the AUC-data and simulated data, respectively.

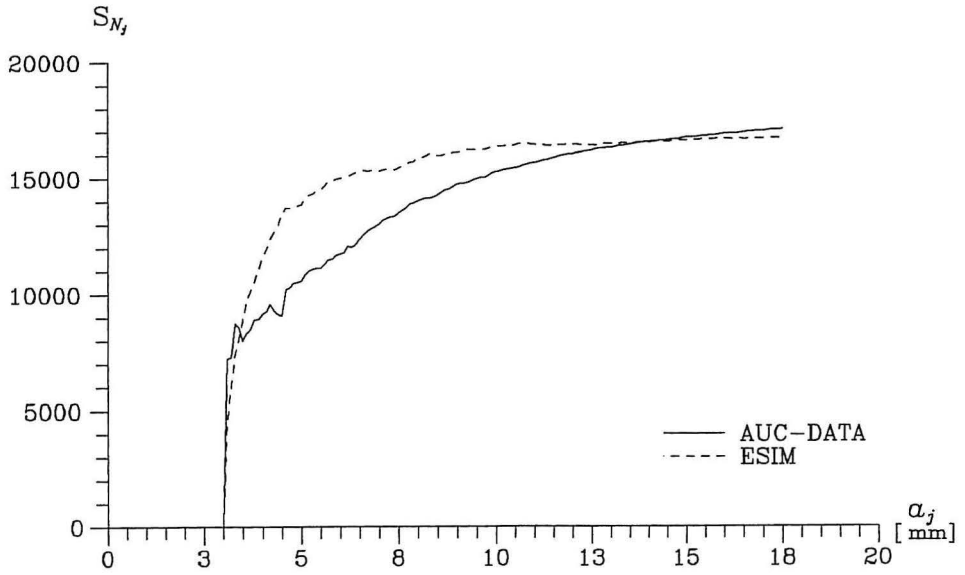

Figure 5.4: Standard deviation of the number of load cycles (S_{N_j}) performed to reach crack the state (a_j), for the AUC-data and the simulated data, respectively. $j = 0, 1, 2, \ldots, 145$, $a_0 = 3.0$ mm and $a_{145} = 17.5$ mm.

The standard deviation of the number of load cycles S_{N_j} applied at a crack state a_j is increasing for increasing crack length, see figure 5.4. The increase is largest for small crack lengths ($a < 5$ mm) after which the standard deviation slowly increases towards a constant value of ≈ 16500. This is most clearly seen for the simulated data. Further, the absolute value of the standard deviation for the simulated data for small crack lengths is larger than for the AUC-data, which can also be seen from figures 5.1 and 5.3. The relative deviation is $\approx 10\%$ for both curves.

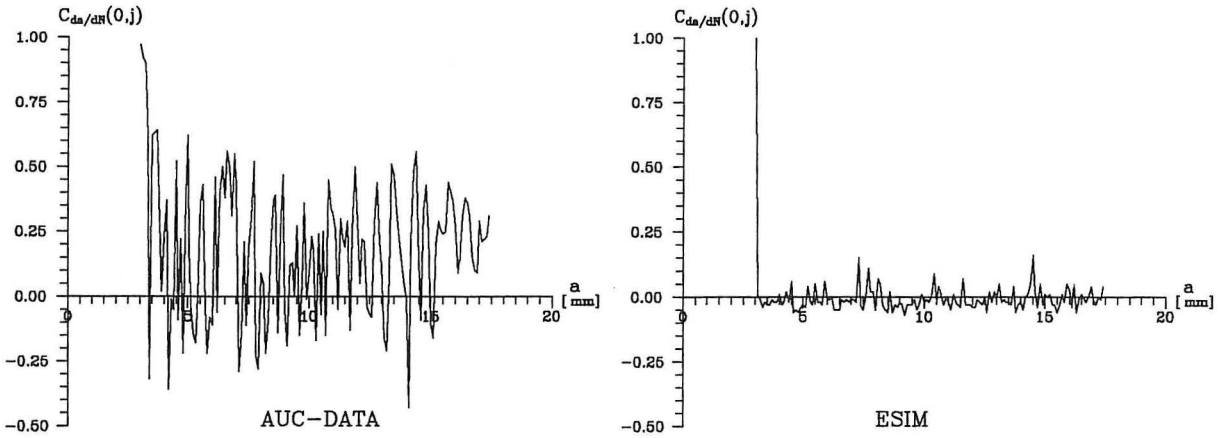

Figure 5.5: Autocovariance of the crack growth rate ($C_{da/dN}$) at the crack state a_0 = 3.0 mm for the AUC-data and ESIM, respectively.

As seen in figure 5.5 the autocovariance $C_{da/dN}(0, j)$ for the AUC-data is concentrated within the interval [-0.25 ; 0.55] which indicates that the crack growth rate throughout the lifetime is highly dependent on the initial crack growth rate. Further, it seems that the mean value is almost constant (≈ 0.15).

The autocovariance $C_{da/dN}(0, j)$ for ESIM fluctuates within a much smaller interval ([-0.075 ; 0.15]) than the AUC-data. This might be due to the different number of curves, i.e. 34 for the AUC-data and 500 for ESIM.

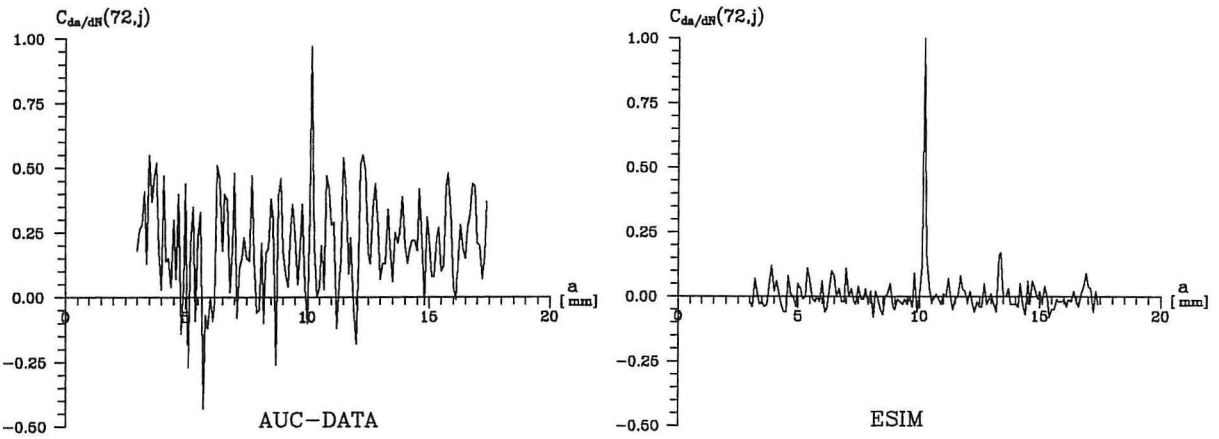

Figure 5.6: Autocovariance of the crack growth rate ($C_{da/dN}$) at the crack state a_{72} = 10.2 mm for the AUC-data and ESIM, respectively.

In figure 5.6 the same tendency as in figure 5.5 is seen. Thus, the autocovariance $C_{da/dN}(72, j)$ for the AUC-data is concentrated within the interval [-0.15 ; 0.50] with constant mean value (≈ 0.20) meaning that the crack growth rate obtained before the crack state $a_{72} = 10.2$ mm influences the crack growth rate at this crack state which again influences the crack growth rate after the crack state $a_{72} = 10.2$ mm.

This influence is not found in the autocovariance $C_{da/dN}(72, j)$ for ESIM. The curve

fluctuates within the interval [-0.075 ; 0.15] with the peak value 1 for $a_{72} = 10.2$ mm as expected.

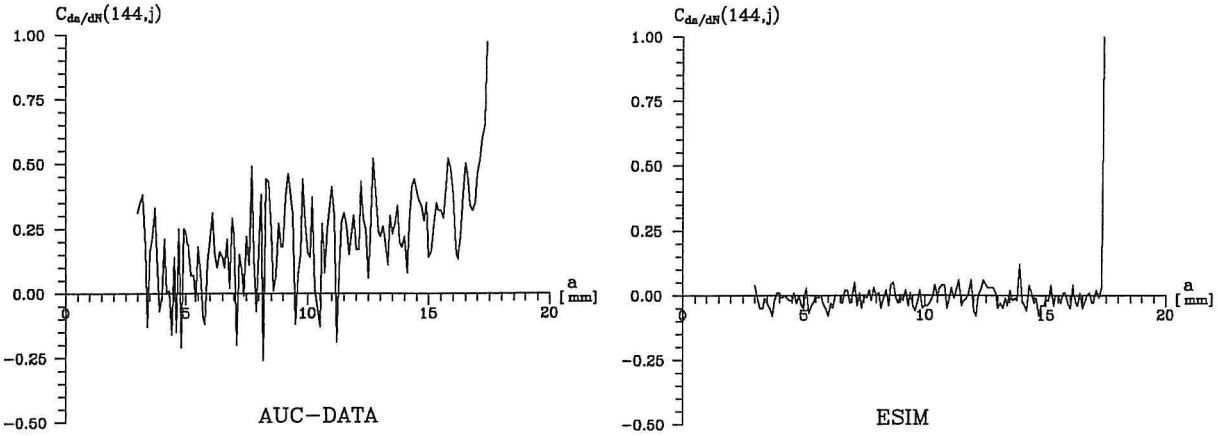

Figure 5.7: Autocovariance of the crack growth rate ($C_{da/dN}$) at the crack state a_{144} = 17.4 mm for the AUC-data and ESIM, respectively.

The autocovariance $C_{da/dN}(144, j)$ for the AUC-data shown in figure 5.7 differs from the ones in figures 5.5 and 5.6 since the mean value increases for increasing crack length. Thus, $C_{da/dN}(144, j)$ starts with values in the interval [-0.20 : 0.25] ending with values in the interval [0.15 ; 0.55].

However, the autocovariance $C_{da/dN}(144, j)$ for ESIM is like the ones in figures 5.5. and 5.6 with small fluctuations within the interval [-0.10 ; 0.10] and with a peak value = 1 at $a_{144} = 17.4$ mm.

These statistical values of the AUC-data are compared with the corresponding values obtained from the simulated data in the quantitative test. The remaining statistical curves are shown in [Gansted, L.; 1991].

The comparison is based on the following norm, which is applied to each of the statistical properties.

$$q_X = \left[\sum_{j=0}^{n} (x_{\text{ESIM}} - x_{\text{AUC}})^2 \right]^{\frac{1}{2}} \tag{5.1}$$

where

X	=	the statistical property in consideration
n	=	number of crack states = 145 for δN_j and 146 for N_j
x_{ESIM}	=	statistical value of the simulated data ESIM
x_{AUC}	=	statistical value of the AUC-data

The calculation of the q-values for the simulated curves shown in figure 5.3 on the basis of table 5.2 (mentioned as ESIM) is given in table 5.5. Further, the norm values for $\delta a = 0.2$ mm and other parameters as in table 5.2 are given for comparison (ESIM 0.2).

	$q_{\overline{\delta N}_j}$ (10^6)	$q_{S_{\delta N_j}}$ (10^7)	$q_{Q_{\delta N_j}}$ (10^6)	$q_{\overline{N}_j}$ (10^9)	$q_{S_{N_j}}$ (10^8)	$q_{Q_{N_j}}$ (10^7)	$q_{C_{da/dN}}$
ESIM	9.1	7.9	134.2	5.1	4.3	0.56	476.8
ESIM 0.2	13.4	25.0	6.60	9.0	76.3	918.7	____

Table 5.5: Norm values q for: mean value ($\overline{\delta N}_j$), standard deviation ($S_{\delta N_j}$) and probability density ($Q_{\delta N_j}$) of the number of load cycles applied at each crack state (a_j); mean value ($\overline{N}_j$), standard deviation (S_{N_j}) and probability density (Q_{N_j}) of the number of load cycles applied to reach a crack state (a_j); autocovariance of the crack growth rate ($C_{da/dN}$) for three different crack lengths. The norm values are calculated for simulated data (ESIM A and ESIM 0.2, respectively) using the AUC-data as reference.

From table 5.5 it is seen that ESIM generally gives smaller norm values than ESIM 0.2, i.e. ESIM is more like the AUC-data. This was to be expected since δa in ESIM is chosen so the value of S_{N_j} equals the value for the AUC-data.

6. CONCLUSIONS

The FMF-model, see chapter 2, is a new numerical cumulative damage model based on fracture mechanics in which the cumulative damage is described by a discrete-time, discrete-state Markov process. The time is measured as numbers of duty cycles, whereas the state of damage is given as a crack length. The crack is assumed to propagate in steps of the length δa.

The evaluation of the FMF-model is based on a comparison of empirical data and numerical data. Both qualitative and quantitative criteria have been used. The criteria are outlined in chapter 3.

Two sets of empirical data have been used as references for the numerical data, see sections 4.1 and 5.1, respectively. The empirical fatigue crack growth data in section 4.1 is a result of tests performed with an aluminium alloy, whereas the series of fatigue crack growth curves in section 5.1 has been performed using a mild steel.

On the basis of the empirical data, the necessary model parameters used in the FMF-model were calculated and simulations of fatigue crack growth data have been performed in sections 4.2 and 5.2, respectively.

The applicability of the FMF-model is evaluated on the basis of the results in sections 4.3 and 5.3. Further, it is discussed if the crack step length can be regarded as a characteristic value of the material as assumed in chapter 2.

The qualitative demand concerning similarity in the form and the progress of the fatigue crack growth curves can be fulfilled if λ - the number of load cycles in a duty

cycle - is small, e.g. $\lambda \leq 100$. Further, the material parameters C and m in Paris' formula (2.3) must be determined from tests with specimens made of material from the same casting as the structure.

The statistical properties of fatigue crack growth data established by simulation correspond to the statistical properties of experimental fatigue data if adequate choices of the model parameters used in the FMF-model are made. In fact, the analyses in sections 4.3 and 5.3 show that the crack step length δa can be regarded as a characteristic value of the material determined by (4.3). This means that the Markov assumption is reasonable for small values of the step length, δa.

Thus, the FMF-model can fulfil both the qualitative and quantitative demand by a careful establishment of the model parameters. One of the main results is that once the material constants in Paris' formula, C and m, and δa are determined, the state of damage in any structure of the given material can be calculated numerically.

REFERENCES

[Benjamin, J.R and C.A. Cornell; 1970]
"Probability, Statistics, and Decision for Civil Engineers"
McGraw-Hill, Inc.

[Bogdanoff, J.L. and F. Kozin; 1985]
"Probabilistic Models of Cumulative Damage"
John Wiley & Sons, Inc.

[Corbly, D.M. and P.F. Packman; 1973]
"On the Influence of Single and Multiple Peak Overloads on Fatigue Crack Propagation In 7075-T6511 Aluminum"
Engineering Fracture Mechanics, Vol.5, No.2, p.479-497
Pergamon Press

[Gansted, L., R. Brincker and L. Pilegaard Hansen; 1991]
"Fracture Mechanical Markov Chain Crack Growth Model"
Engineering Fracture Mechanics, Vol.38, No.6, pp.475-489
Pergamon Press plc.

[Gansted, L.; 1993]
"Fatigue of Steel: Constant-Amplitude Load on CCT-Specimens"
Fracture and Dynamics, Paper No. 49
Aalborg University, Denmark
ISSN 0902-7513 R9344

[Hellan, K.; 1985]
"Introduction to Fracture Mechanics"
McGraw-Hill Book Co. - International Student Edition

[Paris, P.C. and F. Erdogan; 1963]
"A Critical Analysis of Crack Propagation Laws"
Journal of Basic Engineering, Trans ASME Series D 85, p.528-534

[Schijve, J.; 1979]
"Four Lectures on Fatigue Crack Growth"
Engineering Fracture Mechanics, Vol.24, No.11, p.167-221
Pergamon Press Ltd.

[Virkler, D.A., B.M. Hillberry and P.K. Goel; 1979]
"The Statistical Nature of Fatigue Crack Propagation"
Journal of Engineering Materials, Vol.101, No.2, p.148-153, April 1979
American Society of Mechanical Engineers

SYMBOLS

a	=	crack length
a_0	=	initial crack length
a_b	=	failure crack length
δa	=	crack length increment
b	=	failure state
C	=	material constant
C[.]	=	autocovariance of random variable
CCT	=	Center Cracked Tension
CD	=	cumulative damage
d	=	damage state
da	=	crack length increase
dN	=	increase in number of cycles
DC	=	duty cycle
E[.]	=	expected value of random variable
f_Z	=	probability mass function
F	=	geometry and load dependent factor
ΔK	=	stress intensity factor range
ΔK_{eff}	=	effective stress intensity factor range
m	=	material constant
n	=	number of load cycles in a duty cycle
N	=	number of cycles
$\overline{N}$	=	mean value of number of cycles

N_f = number of cycles to cause failure
δN = increase in number of duty cycles
p = $1 - q$
$\overline{p}_0$ = initial state vector
$\overline{p}_x$ = state vector
P[.] = probability distribution of random variable
$\overline{\overline{P}}_i$ = transition matrix for the ith duty cycle
q = transition probability
q[.] = norm value
S[.] = standard deviation of random variable
t_i = time moment, $i = 1, 2$
Var[.] = variance of random variable
x = discrete time
Z = Bernoulli random variable
λ = number of load cycles in one duty cycle
σ_{cl} = crack closure stress
$\sigma_{\max}$ = maximum stress
$\sigma_{\min}$ = minimum stress
$\Delta\sigma$ = stress range
$\Delta\sigma_{\text{eff}}$ = effective stress range

FRACTURE AND DYNAMICS PAPERS

PAPER NO 24: Jens Peder Ulfkjær, Rune Brinker & Steen Krenk: *Analytical Model for Complete Moment-Rotation Curves of Concrete Beams in bending.* ISSN 0902-7513 R9021.

PAPER NO 25: Leo Thesbjerg: *Active Vibration Control of Civil Engineering Structures under Earthquake Excitation.* ISSN 0902-7513 R9027.

PAPER NO. 26: Rune Brincker, Steen Krenk & Jakob Laigaard Jensen: *Estimation of correlation Functions by the Random Dec Technique.* ISSN 0902-7513 R9028.

PAPER NO. 27: Jakob Laigaard Jensen, Poul Henning Kirkegaard & Rune Brincker: *Model and Wave Load Identification by ARMA Calibration.* ISSN 0902-7513 R9035.

PAPER NO. 28: Rune Brincker, Steen Krenk & Jakob Laigaard Jensen: *Estimation of Correlation Functions by the Random Decrement Technique.* ISSN 0902-7513 R9041.

PAPER NO. 29: Poul Henning Kirkegaard, John D. Sørensen & Rune Brincker: *Optimal Design of Measurement Programs for the Parameter Identification of Dynamic Systems.* ISSN 0902-7513 R9103.

PAPER NO. 30: L. Gansted & N. B. Sørensen: *Introduction to Fatigue and Fracture Mechanics.* ISSN 0902-7513 R9104.

PAPER NO. 31: R. Brincker, A. Rytter & S. Krenk: *Non-Parametric Estimation of Correlation Functions.* ISSN 0902-7513 R9120.

PAPER NO. 32: R. Brincker, P. H. Kirkegaard & A. Rytter: *Identification of System Parameters by the Random Decrement Technique.* ISSN 0902-7513 R9121.

PAPER NO. 33: A. Rytter, R. Brincker & L. Pilegaard Hansen: *Detection of Fatigue Damage in a Steel Member.* ISSN 0902-7513 R9138.

PAPER NO. 34: J. P. Ulfkjær, S. Krenk & R. Brincker: *Analytical Model for Fictitious Crack Propagation in Concrete Beams.* ISSN 0902-7513 R9206.

PAPER NO. 35: J. Lyngbye: *Applications of Digital Image Analysis in Experimental Mechanics.* Ph.D.-Thesis. ISSN 0902-7513 R9227.

PAPER NO. 36: J. P. Ulfkjær & R. Brincker: *Indirect Determination of the $\sigma - w$ Relation of HSC Through Three-Point Bending.* ISSN 0902-7513 R9229.

PAPER NO. 37: A. Rytter, R. Brincker & P. H. Kirkegaard: *An Experimental Study of the Modal Parameters of a Damaged Cantilever.* ISSN 0902-7513 R9230.

PAPER NO. 38: P. H. Kirkegaard: *Cost Optimal System Identification Experiment Design.* ISSN 0902-7513 R9237.

PAPER NO. 39: P. H. Kirkegaard: *Optimal Selection of the Sampling Interval for Estimation of Modal Parameters by an ARMA-Model.* ISSN 0902-7513 R9238.

FRACTURE AND DYNAMICS PAPERS

PAPER NO. 40: P. H. Kirkegaard & R. Brincker: *On the Optimal Location of Sensors for Parametric Identification of Linear Structural Systems.* ISSN 0902-7513 R9239.

PAPER NO. 41: P. H. Kirkegaard & A. Rytter: *Use of a Neural Network for Damage Detection and Location in a Steel Member.* ISSN 0902-7513 R9245

PAPER NO. 42: L. Gansted: *Analysis and Description of High-Cycle Stochastic Fatigue in Steel.* Ph.D.-Thesis. ISSN 0902-7513 R9135.

PAPER NO. 43: M. Krawczuk: *A New Finite Element for Static and Dynamic Analysis of Cracked Composite Beams.* ISSN 0902-7513 R9305.

PAPER NO. 44: A. Rytter: *Vibrational Based Inspection of Civil Engineering Structures.* Ph.D.-Thesis. ISSN 0902-7513 R9314.

PAPER NO. 45: P. H. Kirkegaard & A. Rytter: *An Experimental Study of the Modal Parameters of a Damaged Steel Mast.* ISSN 0902-7513 R9320.

PAPER NO. 46: P. H. Kirkegaard & A. Rytter: *An Experimental Study of a Steel Lattice Mast under Natural Excitation.* ISSN 0902-7513 R9326.

PAPER NO. 47: P. H. Kirkegaard & A. Rytter: *Use of Neural Networks for Damage Assessment in a Steel Mast.* ISSN 0902-7513 R9340.

PAPER NO. 48: R. Brincker, M. Demosthenous & G. C. Manos: *Estimation of the Coefficient of Restitution of Rocking Systems by the Random Decrement Technique.* ISSN 0902-7513 R9341.

PAPER NO. 49: L. Gansted: *Fatigue of Steel: Constant-Amplitude Load on CCT-Specimens.* ISSN 0902-7513 R9344.

PAPER NO. 50: P. H. Kirkegaard & A. Rytter: *Vibration Based Damage Assessment of a Cantilever using a Neural Network.* ISSN 0902-7513 R9345.

PAPER NO. 51: J. P. Ulfkjær, O. Hededal, I. B. Kroon & R. Brincker: *Simple Application of Fictitious Crack Model in Reinforced Concrete Beams.* ISSN 0902-7513 R9349.

PAPER NO. 52: J. P. Ulfkjær, O. Hededal, I. B. Kroon & R. Brincker: *Simple Application of Fictitious Crack Model in Reinforced Concrete Beams. Analysis and Experiments.* ISSN 0902-7513 R9350.

PAPER NO. 53: P. H. Kirkegaard & A. Rytter: *Vibration Based Damage Assessment of Civil Engineering Structures using Neural Networks.* ISSN 0902-7513 R9408.

PAPER NO. 54: L. Gansted, R. Brincker & L. Pilegaard Hansen: *The Fracture Mechanical Markov Chain Fatigue Model Compared with Empirical Data.* ISSN 0902-7513 R9431.

Department of Building Technology and Structural Engineering
Aalborg University, Sohngaardsholmsvej 57, DK 9000 Aalborg
Telephone: +45 98 15 85 22 Telefax: +45 98 14 82 43